Available on CMS information server

CMS CR 2006/057

CMS Conference Report

September 11, 2006

Beyond Standard Model Physics at the Large Hadron Collider at CERN

R. Alemany-Fernandez

CMS Collaboration

Abstract

This conference report presents a compilation of some of the latest results on prospects for Extra Dimensions and Heavy Bosons Models with A Toroidal LHC ApparatuS (ATLAS) and the Compact Muon Solenoide (CMS). ATLAS and CMS are two general purpose detectors placed at two equidistant points in the Large Hadron Collider (LHC) at CERN. The results presented here correspond, in most of the cases, to full simulation and full reconstruction of the hadron interactions at $\sqrt{s}$ = 14 TeV and to low and/or high luminosity. In general, theoretical and systematic uncertainties are considered in the final results.

Presented at *Physics at LHC,* Cracow Poland, July 3-8, 2006

To be submitted to *Physics at LHC Conference Proceedings*

1 Introduction

Theorists argue in different ways that there should exist physics Beyond the Standard Model (BSM). This is one of the reasons why the Large Hadron Collider (LHC) and its detectors are being built at CERN.

In this conference report, the most recent results, from the experimental (simulation) point of view, on Extra Dimensions and Extra Gauge Bosons will be reviewed. In particular, the Compact Muon Solenoide (CMS) and the A Toroidal LHC ApparatuS (ATLAS) Collaborations analyses will be considered here. The last section of this chapter will be devoted to an extremely important subject: once a signature is discovered in the detector, how we can distinguish which model is the responsible for it. This issue gets raised because many beyond standard model scenarios (including Supersymmetry) predict the same kind of topologies, although the discrimination between Supersymmetry and other BSM models will not be addressed here.

Before reviewing the LHC results on BSM physics, it is worth to spend a few words talking about another very important matter related with theoretical and experimental uncertainties. Theoretical uncertainties from Parton Distribution Functions (PDF), hard process scale (Q^2), differences between Next-to-Next-to-Leading Order, Next-to-Leading Order and Leading Order calculations, and many more, affect the signal and background magnitudes, the efficiency of the selection cuts, the significance computation, etc.

On the other hand, systematic uncertainties associated with the detector measurements like luminosity, track and vertex reconstruction efficiency (very much influenced by the quality of the alignment), particle energy reconstruction (which also has a systematic uncertainty component coming from a misaligned tracker detector), drift time and drift velocities uncertainties, etc; also affect the background and signal modifying the final results. Therefore is very important to try to quantify, whenever is possible, the systematic uncertainties and discuss the way they modify the final numbers, as most of the analysis presented here does.

This document is organized as follows: Section two is devoted to Extra Dimensional Models; Section three to Heavy Bosons theories; Section four explains some ways of distinguishing among different BSM signatures; finally Section five contains the Conclusions.

2 Extra Dimensional Models

2.1 Introduction

The main motivation for the development of theories beyond the Standard Model is the hierarchy problem, i. e., why the gravity energy scale (or Planck Mass, M_{Pl}) and the electroweak energy scale (M_{EW}) are so different: $\sim 10^{19}$ GeV compared to $\sim 10^{3}$ GeV, respectively. Several possibilities have been suggested to solve this "naturality" problem: perturbative solutions like Supersymmetry; and non-perturbative solutions like Compositeness and Technicolor. Alternatively, one can exploit the geometry of space-time via Extra Dimensional Theories.

In this section the following four models will be reviewed: Arkani-Dimopoulos-Dvali (ADD) Model, Randall-Sundrum (RS) or warped extra dimensions, TeV^{-1} size extra dimensions and Universal Extra Dimensions (UED).

2.2 The ADD Model

2.2.1 Theoretical motivation

According to this model [1], M_{Pl} is not a fundamental scale, but M_{EW} (since it is an experimental certainty), which also sets the scale for the strength of the gravitational interactions, and as a consequence, the ultra violet cut-off of the theory is $\sim M_{EW}$. But then, how can the usual strength of gravitation arise in such a picture? The solution consists of postulating the existence of δ extra dimensions of radius R were gravity propagates. In our four dimensional world, the graviton is seen as an infinite tower of Kaluza-Klein (KK) states (n denotes the KK level). The model parameters are: δ (the number of extra dimensions) and $M_{Pl(4+\delta)}$ (the Planck mass in the $4+\delta$ dimensions that is a fundamental scale above which new physics enters and modifies the results). $M_{Pl(4+\delta)}$ is related to R and the four dimensional Planck mass through the following expression:

$$M^2_{Pl} \sim M^{2+\delta}_{Pl(4+\delta)} R^{\delta} \qquad \text{(Eq. 1)}$$

For $M_{Pl} \sim 10^{19}$ GeV and $M_{Pl(4+\delta)} \sim M_{EW}$, the value of the compactification radius is $R \sim 10^{32/\delta}\ 10^{-17}$ cm. There exist already some constraints on the parameters:

- For $\delta = 1 \rightarrow R \sim 10^{13}$ m. This value is already ruled out because deviations from Newtonian gravity over solar distances have not been observed.
- For $\delta = 2 \rightarrow R \sim 1$ mm. This value is not very likely because of cosmological arguments. The closest allowed $M_{Pl(4+\delta)}$ value for $\delta = 2$ is ~ 30 TeV, out of the LHC reach.
- $\delta > 6$ may be difficult to be probed at LHC because the cross-sections are very low.
- Finally, TEVATRON limit is: $M_{Pl(4+\delta)} > 1$ TeV [2].

Since the mass of the Kaluza-Klein graviton of any KK level (n), $m(G_n^{KK})$, is proportional to n/R and, according to the above limits, the compactification radius is of the order of the mm or below, ADD models are characterized by light gravitons. The mass difference between gravitons of consecutive KK levels is between eV and MeV. The graviton couplings are proportional to M_{Pl}^{-1}, but given that graviton masses are very small, a high density of KK modes are produced, and therefore the cross-section of the process gets enhanced and its signature can be seen in the detectors.

2.2.2 Experimental results

There are two ways of producing KK gravitons in ADD models: via direct graviton production and via virtual exchange.

Direct graviton production:

ATLAS results for pp → jet+G^{KK} [3]: the topology consists of a jet with high transverse energy ($E_T > 500$ GeV), and a high missing transverse energy ($E_T^{miss} > 500$ GeV) from the escaping gravitons. The analysis also vetoes the leptons via isolation and identification criteria. The irreducible SM background consists of *jet* $Z \rightarrow$ *jet* $\nu\,\nu$ and *jet* $W \rightarrow$ *jet* $l\,\nu$. The signal and background was generated with ISAJET; the PDF used was CTEQ3L; the analysis was based on fast simulation and reconstruction. Figure 1 shows the E_T^{miss} for the different signals and backgrounds for 100 fb^{-1} of integrated luminosity and $\sqrt{s} = 14$ TeV. For $S/\sqrt{B} > 5$ (S and B are the number of signal and background events, respectively, that pass the selection criteria), with $S > 100$ and $E_T^{jet} > 1$ TeV the following discovering limits are achieved: $M_{Pl(4+\delta)}$ (= M_D in the plot) = 7.7 : 6.2 : 5.2 for δ = 2 : 3 : 4, respectively.

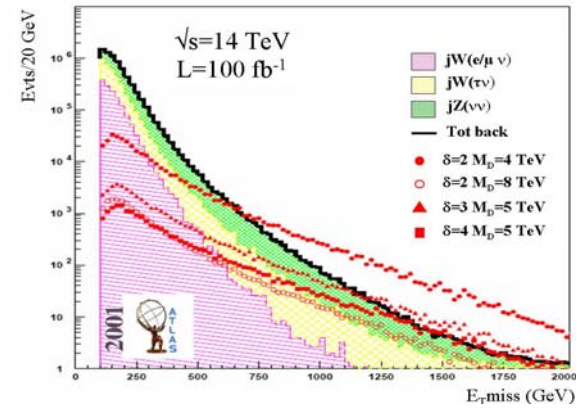

Figure 1: E_T^{miss} for different ADD signals (different values of the parameter space) with jet and missing transverse energy in the final state and the corresponding irreducible backgrounds.

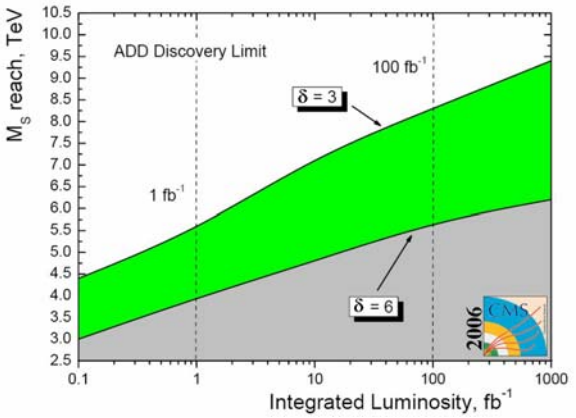

Figure 2: ADD discovery limit for graviton virtual production with 2 muons in the final state for different values of the number of extra dimensions (δ).

CMS results for pp → γ+G^{KK} [4,5]: Another inte-resting signal at LHC is the production of a G^{KK} in association with a photon. Although the rates are much lower than in the jet case, and the region (δ,$M_{Pl(4+\delta)}$) which can be probed is much more limited, this signature could be used as a confirmation after the discovery in the jet channel.

This topology will not be detectable in the low p_T region because the cross-section of the background, in particular the irreducible one, is too large. Therefore, a minimum $p_T > 400$ GeV is consistently requested. The topology consists of a high E_T photon, produced in the central pseudo-rapidity region and back-to-back with respect to the missing transverse energy from the undetected gravitons. The irreducible SM background is $Z\gamma \rightarrow \nu\nu\gamma$. Other backgrounds also considered in this analysis are: $W \rightarrow e(\mu,\tau)\nu$, $W\gamma \rightarrow e\nu\,\gamma$, γ+jets, QCD, di-γ, Z^0+jets. The estimated rates for cosmic muons (the biggest background in CDF) and beam halo muons for a $p_T >$

400 GeV is 11 Hz and 1 Hz respectively. Those backgrounds have not been considered in the CMS analysis yet. The signal was generated with PYTHIA and compared to the SHERPA generator. The backgrounds were generated with PYTHIA and compared to SHERPA, CompHEP and Madgraph. The PDF used was CTEQ6L. The results given in Tab. 1 correspond to full simulation and reconstruction, with the significance calculated according to the expression [6]:

$$\mathcal{S} = 2(\sqrt{(S+B)} - \sqrt{B}) > 5 \qquad \text{(Eq. 2)}$$

The 5σ discovery reach of $M_{Pl(4+\delta)} > 3.5$ TeV is not possible when including theoretical uncertainties.

Table 1: Integrated luminosity needed in CMS for a 5σ significance discovery of the different parameter space values of the direct production of gravitons in the γ and missing energy final state.

$M_{Pl(4+\delta)}/\delta$	2	3	4	5	6
1.0 TeV	0.21 fb^{-1}	0.16 fb^{-1}	0.14 fb^{-1}	0.15 fb^{-1}	0.15 fb^{-1}
1.5 TeV	0.83 fb^{-1}	0.59 fb^{-1}	0.56 fb^{-1}	0.61 fb^{-1}	0.59 fb^{-1}
2.0 TeV	2.8 fb^{-1}	2.1 fb^{-1}	1.9 fb^{-1}	2.1 fb^{-1}	2.3 fb^{-1}
2.5 TeV	9.9 fb^{-1}	8.2 fb^{-1}	8.7 fb^{-1}	9.4 fb^{-1}	10.9 fb^{-1}
3.0 TeV	47.8 fb^{-1}	46.4 fb^{-1}	64.4 fb^{-1}	100.8 fb^{-1}	261.2 fb^{-1}
3.5 TeV	5σ discovery not possible anymore when including theoretical systematic uncertainties				

Virtual production of gravitons:

CMS results for $pp \rightarrow G^{KK} \rightarrow \mu\mu$ [5,7]: the topology consists of two opposite signed muons with an invariant mass above 1 TeV. The cross-section is the sum of the SM contribution, the extra dimensional contribution and an interference term that is a function of the energy scale of the theory, the number of extra dimensions and the centre of mass energy. The irreducible background is the Drell-Yan production of two muons. Other backgrounds also considered are ZZ, WZ, WW and tt, but they are successfully suppressed after the selection cuts.

The signals were generated at Leading Order in perturbation theory with a K factor of 1.38. STAGEN and PYTHIA generators were used with initial and final state radiation. The PDF taken into account was CTEQ6L. The signals and backgrounds were fully simulated and reconstructed. The following systematic uncertainties were taken into consideration: theoretical uncertainties, muon and tracker misalignment and trigger uncertainties. Figure 2 shows the $M_{Pl(4+\delta)}$ (M_S in the plot) 5σ significance discovery reach, with $\mathcal{S}$ computed according to Eq. 2 for different values of the number of extra dimensions.

2.3 The RS Model

2.3.1 Theoretical motivation

RS models [8] postulate that gravity propagates in a 5 dimensional bulk (therefore δ=1) of finite extent with two rigid boundaries of (3+1) dimensions that extend infinitely. The SM fields are constraint on one of the 3-branes (y=Rπ where y is the extra dimensional coordinate and R is the compactification radius) as depicted in Fig. 3. The mass of the Kaluza-Klein gravitons is given by the following expression:

$$m(G_n^{KK}) = kx_n e^{-kR\pi} = x_n(k/\mathbf{M_{Pl}})\Lambda_\pi \sim \text{TeV} \qquad \text{(Eq. 3)}$$

where k is a scale of the order of the Planck scale, x_n are the roots of the Bessel function of order 1, $\mathbf{M_{Pl}}$ is the reduced Planck mass and Λ_π is the scale of physical processes in the TeV brane. In RS models the gravitons are heavy compared with ADD theories. The graviton coupling is also different with respect to ADD models, being proportional to Λ_π^{-1} for KK levels above the fundamental level (n ≥1). For n=0 the graviton couples with gravitational strength.

The model parameters are: Λ_π and $c = k/\mathbf{M_{Pl}}$. The width of the resonances are controlled by c, the lower the c the narrow the resonances as can be seen in Fig. 4 that shows the Drell-Yan production of different modes of the G^{KK} for different values of c.

2.3.2 Experimental results

CMS results for $pp \rightarrow G_1^{KK} \rightarrow ee, \mu\mu, \gamma\gamma$ [5,9]: at the LHC the RS G_1^{KK} (the first KK excitation of the graviton) would be seen as di-fermion or di-boson resonances, since the coupling of each KK mode is only ~TeV suppressed as discussed in the previous section. Figure 5 shows the $M(G_1^{KK})$ reach for di-electrons, di-photons and di-muons final states for different values of c and integrated luminosity. The region of interest is the one to the left of the curve $\Lambda_\pi < 10$ TeV (which is theoretically preferred [10]) and up to c = 0.1 because c > 0.1 is disfavoured on theoretical grounds as the bulk curvature becomes too large (larger than the 5-dim Planck

scale). The 5σ significance discover areas are the regions to the left of the straight lines. The sensitivity to G_1^{KK} mass is calculated using the likelihood estimator [11] based on event counting suited for small event samples:

$$\mathcal{S} = \sqrt{(2[(S+B)\log(1+S/B)-S])} > 5 \qquad \text{(Eq. 4)}$$

The CMS analysis is based on full simulation and reconstruction, and includes the study of theoretical and experimental systematic uncertainties. As an example, Fig. 5 on the right shows the one sigma theoretical and experimental systematic uncertainties influence on the discovery limit. The misalignment scenario taken into account in the result corresponds to the first period of detector alignment obtained with ~ $1fb^{-1}$ of data. During this period the muon reconstruction efficiency will be unaffected, while the momentum resolution will be reduced from 1-2% to 4-5%.

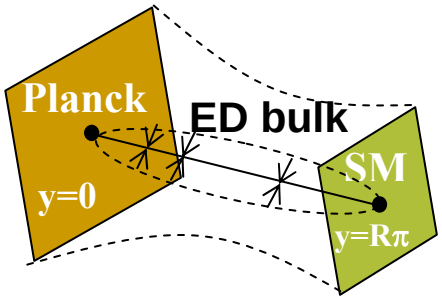

Figure 3: Schematic representation of the RS model geometry.

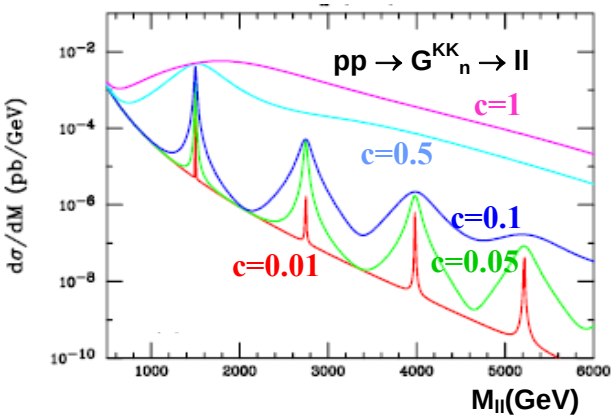

Figure 4: Drell-Yan production of a 1.5 TeV RS G^{KK} and its subsequent tower states for different values of c. The x axis is the invariant mass of the pair of leptons in the final state.

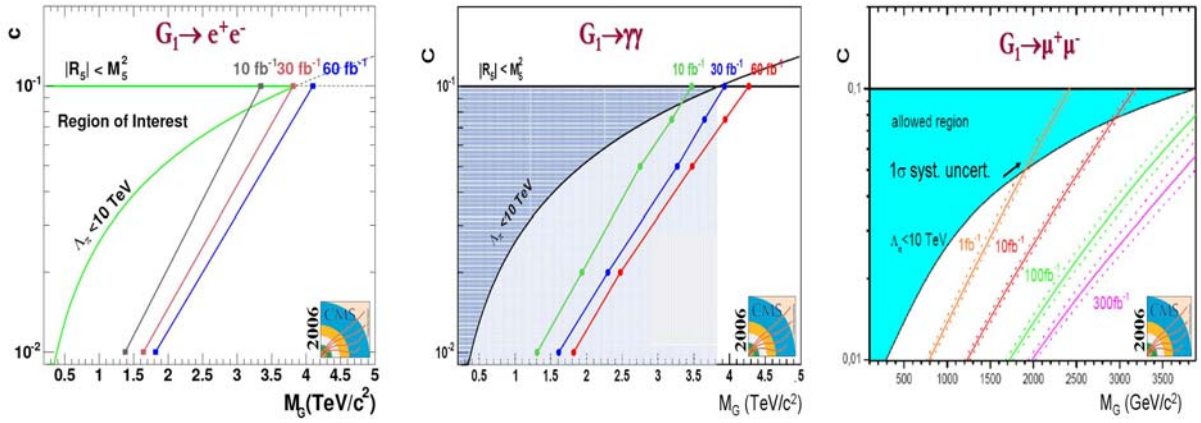

Figure 5: $M(G_1^{KK})$ reach for di-electrons, di-photons and di-muons final states, respectively, for different values of c and integrated luminosity. The 5σ significance discovery is the region to the left of the coloured lines. The di-muon plot also shows the 1σ theoretical and experimental uncertainty on the integrated luminosity needed to reach the 5σ significance.

2.4 The TeV^{-1} size Model

2.4.1 Theoretical motivation

An interesting variation to the ADD model assumes that only the fermions are confined in the 3-brane, whereas the gauge fields propagates also in a number of additional small extra dimensions orthogonal to the brane with R ~ 1 TeV^{-1} [12]. The characteristic signature of these models is KK excitations of the gauge bosons appearing in the detectors as resonances. Depending on the assumptions made, there are different scenarios. The results shown in the following assume that:

- The Higgs is in the bulk; the fundamental mode of the Higgs field acquires a VEV producing spontaneous symmetry breaking, thus the mass matrix of the gauge fields is diagonal and given by:

$$m(gauge^{KK}{}_n) = [m_0{}^2+(n/R)^2]^{1/2} \quad \text{(Eq. 5)}$$

where m_0 is the VEV induced mass of the gauge 0 mode.

- $\delta = 1$.
- The fermion fields are localized at specific points in the TeV^{-1} dimension but not on a rigid brane (this is convenient assumption since it suppresses a number of dangerous processes). This assumption gives rise to two possible models:

  - **M1**: all SM fermions localized in the same orbifold point and as a consequence, the KK gauge states couplings to SM fermions are the same as the SM ones but scaled by a factor √2. This gives rise to a destructive interference between the SM gauge bosons and the KK excitations.

  - **M2**: the quarks and leptons are localized at opposite fixed orbifold points giving rise to a constructive interference.

The effect of the interference can be seen in Fig. 6 taken from [13] which shows the invariant mass distribution of the electron pair produced in the process $pp \rightarrow Z_1{}^{KK}/\gamma_1{}^{KK} \rightarrow e^+e^-$ for the M1 (dashed) and M2 (dotted) models compared with the SM background (solid line).

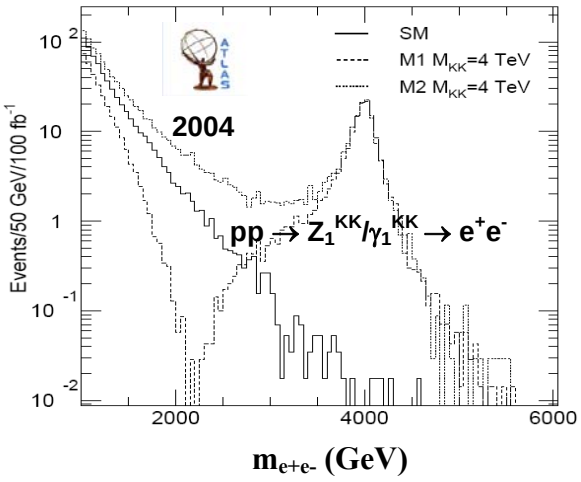

Figure 6: Invariant mass distribution of the electron pair produced in the process $pp \rightarrow Z_1{}^{KK}/\gamma_1{}^{KK} \rightarrow e^+e^-$ for models M1 (dashed) and M2 (dotted) compared with the Standard Model background (solid line).

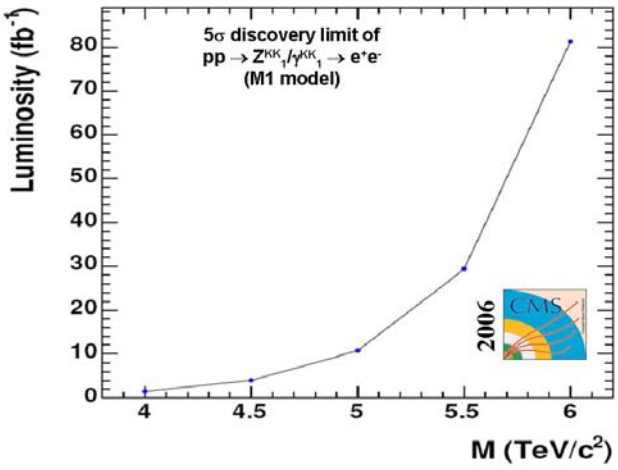

Figure 7: Five sigma discovery limit of the $Z^{KK}{}_1/\gamma^{KK}{}_1$ in the M1 TeV^{-1} Extra Dimensional model. The x-axis is the compactification scale ($M=R^{-1}$) and the y-axis is the integrated luminosity needed to reach a 5σ discovery. The signal is $pp \rightarrow Z^{KK}{}_1/\gamma^{KK}{}_1 \rightarrow e+e-$.

2.4.2 Experimental results

CMS results for $pp \rightarrow Z_1{}^{KK}/\gamma_1{}^{KK} \rightarrow ee$ [5,9:e+e-]: the topology of this signature consists of two high p_T and isolated electrons. The electromagnetic energy associated to the electron candidate is corrected, among other things, for the energy leak in the hadronic calorimeter and for the ECAL electronics saturation (because of the limited dynamic range of the Multi-Gain-Pre-Amplifier). The saturation takes place for energies above 1.7 TeV in the barrel and 3 TeV in the end-caps. The irreducible background is the Drell-Yan production of a pair of electrons.

The signal and background were generated with an external generator and PYTHIA. For inner bremsstrahlung production the program PHOTOS is used. Then the signal and background are fully simulated and reconstructed with pile-up at low luminosity (~ 10^{33} $cm^{-2}s^{-1}$). Theoretical systematic uncertainties were also studied in detail.

The discovery potential of the compactification scale is determined using Eq. 4. The results are shown in Fig. 7. As can be seen, with an integrated luminosity of ~ 80 fb^{-1}, CMS will be able to detect a peak in the e+e- invariant mass distribution if the compactification scale is below 6 TeV.

ATLAS results for $pp \rightarrow Z_1{}^{KK}/\gamma_1{}^{KK} \rightarrow ll$ (l=e,μ) [13]: ATLAS also performed a detailed study of the leptonic signatures for the production of $Z_1{}^{KK}/\gamma_1{}^{KK}$. The production and decay of the first excitations were fully simulated,

including initial state QCD radiation, and the resulting particles were passed through a parameterized simulation of the ATLAS detector. The 5 sigma significance expression used to compute the results is the following:

$$\mathcal{S} = (S-B)/\sqrt{B} > 5 \text{ with } S > 10 \qquad \text{(Eq. 6)}$$

It was found that with an integrated luminosity of 100 fb^{-1}, ATLAS will be able to detect a peak in the lepton-lepton invariant mass if the compactification scale is below 5.8 TeV.

ATLAS results for pp $\rightarrow W_1^{KK} \rightarrow l\nu$ [14]: The selection cuts to search for $W_1^{KK} \rightarrow l\nu$ events consist of requiring one high p_T and isolated lepton (> 200 GeV) uniquely identified as an electron or muon. The events are also characterized by a high transverse momentum imbalance. The invariant mass of the pair (l,ν) should be larger than 1 TeV. A jet veto algorithm is also applied. The irreducible background is the SM production of $W \rightarrow l\nu$, other backgrounds also considered in the analysis but successfully suppressed were tt, WW, ZZ and WZ.

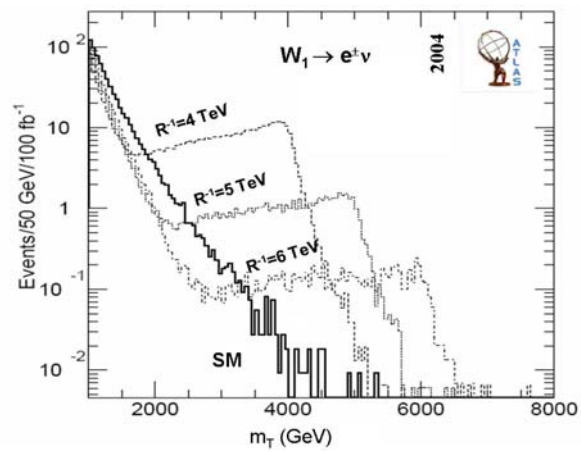

Figure 8: invariant transverse mass distribution of $e^{\pm}\nu$, for the M1 model, for different values of the compactification scale (R^{-1}). The histograms are normalized to 100 fb^{-1}.

The 5σ significance expression used to compute the discovery limit is the one given in Eq. 6 with at least 10 events summed over the two lepton flavours. Figure 8 shows the invariant transverse mass distribution of $e^{\pm}\nu$, for the M1 model, for different values of the compactification scale (R^{-1}). The histograms are normalized to 100 fb^{-1}. It is found that with an integrated luminosity of 100 fb^{-1} the ATLAS detector will be able to detect a peak in the lepton-neutrino invariant transverse mass if $R^{-1} < 6$ TeV.

ATLAS results for pp $\rightarrow g_1^{KK} \rightarrow$ bb\bar, tt\bar [15]: The presence of gluon excitations is detected by analyzing deviations in the di-jet cross-section. An alternative proposal by ATLAS is detecting g_1^{KK} by analyzing its decays to heavy quarks. The two b's final state topology is selected requesting two b-tagged jets with p_T^b cut which is a function of the $m(g_1^{KK})$. In the case of the g_1^{KK} decaying into two tops, one top is forced to follow a leptonic decay. Therefore the selection criteria request a lepton with $p_T^l > 25$ GeV, $E_T^{miss} > 25$ GeV, and two b-tagged jets (from the decay of the second top) with $\Delta R(b1(2)\text{-lep}) < 2(>2)$, and a p_T^b cut which is a function of the $m(g_1^{KK})$. The SM backgrounds taken into account were bb\bar, tt\bar, 2 jets and W+jets.

The events were generated with PYTHIA. The fast simulation and reconstruction programs of ATLAS were used to perform the analysis.

The best discovery potential is achieved with the tt\bar channel and corresponds to $R^{-1} = 3.3$ TeV for 300 fb^{-1} of accumulated data. Although this limit cannot compete with the di-jet channel, the decay into two tops could be used to confirm the presence of a g_1^{KK} in case that an excess of events is observed in the di-jet channel.

2.5 Universal Extra Dimensions

2.5.1 Theoretical motivation

The UED model [16] is an extension of the ADD model in which all the SM fields, fermions as well as bosons, propagate in the bulk, so that each SM particle has an infinite tower of KK partners. The spin of the KK particles is the same as their SM partners, as well as the strength of the couplings. In this paper results of two different scenarios of UED theories are presented. One is the minimal UED (mUED) in which the fields of the theory propagate in a single extra dimension compactified in an orbifold (S^1/Z^2) of size R. The KK-parity is a conserved quantum number which has important phenomenological implications:

- the lightest massive KK particle is the photon and it is stable (dark matter candidate);
- the level one KK states must be pair produced.

mUED is an effective theory valid up to a cut-off scale Λ at which matches another more fundamental theory. Within a given KK level all the particles are degenerated in mass except if radiative corrections are included as sketched in Fig. 9.

The model parameters are: the compactification radius, R; the cut-off scale, Λ; and the Higgs boson mass, m_h. Bounds to the compactification scale already exist. Precision electroweak data measurements set a lower bound of $R^{-1} > 300$ GeV [16]. On the other hand, dark matter constraints imply that $R^{-1} \in [600,1050]$ GeV [17].

The other UED scenario is the fat brane model which postulates that the SM brane is endowed with a finite thickness in the extra dimensions. Gravity-matter interactions break KK number conservation giving the following phenomenological implications:

- the first KK level states decay to a graviton and a SM particle;
- after including radiative corrections the mass degeneracy is broken and photons and leptons are produced.

2.5.2 Experimental results

CMS results for pp → $g_1^{KK} g_1^{KK}$ / $Q_1^{KK} Q_1^{KK}$ / $g_1^{KK} Q_1^{KK}$ → 4 l + *m* jets + 2 γ_1^{KK} [18]: the decay chain chosen in this analysis is the one highlighted with thick arrows in Fig. 9. Only the light quarks (u_1 and d_1 with both quiralities) have been simulated. The final state consists of four low p_T isolated leptons (two pairs of opposite signed same flavour leptons), a *m* number of jets and missing transverse energy from the two undetected γ_1. To improve the background rejection over the signal b-tagging and Z-tagging vetoes are applied. The irreducible backgrounds are *tt+m jets, 4b, ZZ* and *Zbb*. A study at the parton level indicated that other backgrounds, such as ttbb, Zcc, Zcc+m jets and WWZ, either have negligible cross-sections or can be suppresed by basic kinematical cuts.

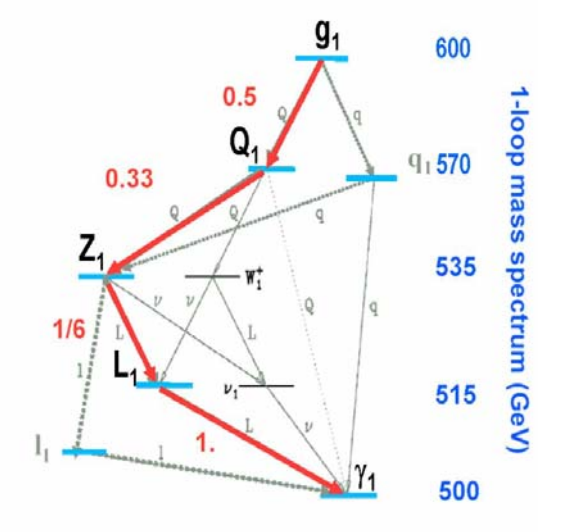

Figure 9: In mUED models mass degeneracy within a KK level is broken by radiative corrections. The decay channel studied by the CMS collaboration is indicated with thick arrows.

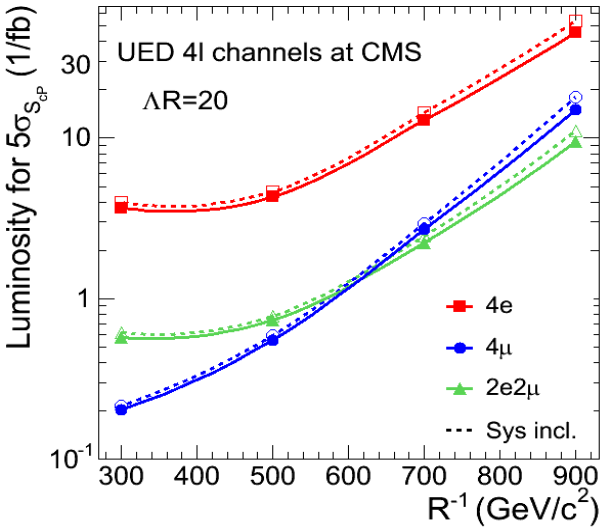

Figure 10: Required luminosity for a 5σ discovery in CMS of UED signals in the 4*l* channel. The systematic uncertainty corresponds to the level of 10-30 fb^{-1}. Additional systematic uncertainties expected in the initial phase (< 1 fb^{-1}) are not included.

Signal events were simulated with CompHEP at leading order (LO). In the cross section calculation the QCD scale was set to 2/R, the radiative corrections were also evaluated at 2/R and the CTEQ5L parton distribution functions (PDF) were used. The dedicated program UEDDECAY-3.00 was used to decay the KK particles. Only the decays that allow the production of four lepton final states were switched on. The ZZ and Zbb background event samples were simulated with CompHEP and Pythia. Top and bottom samples were generated with Alpgen. The NLO values of the cross-section have been applied to all background samples. Then the signal and background were fully simulated and reconstructed. The study was performed for the LHC run at low luminosity (~ $2x10^{33}$ $cm^{-2}s^{-1}$) including theoretical and systematic uncertainties.

The discovery sensitivity for different values of the parameter space and different luminosities is shown in Fig. 10. A common significance estimator was used, ScP [19]. The ScP gives the probability from Poisson distribution with mean B to observe equal or greater than S+B events, converted to the equivalent number of standard deviations of a Gaussian distribution. If B is too small the ScP is approxiamed by Eq. 2.

ATLAS results for pp → $g_1^{KK} g_1^{KK}$ / $Q_1^{KK} Q_1^{KK}$ / $g_1^{KK} Q_1^{KK}$ → 2 jets + 2 G^{KK} [20]: the topology of these processes consists of two back-to-back energetic jets and large missing transverse energy from the undetected

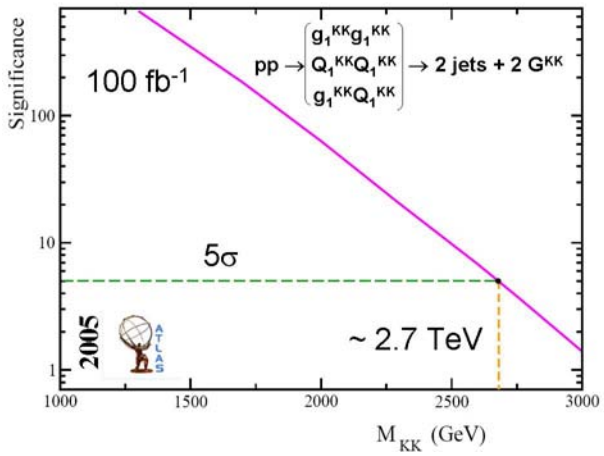

Figure 11: variation of the significance of the signal as a function of the mass of the first KK excitation state for 100 fb^{-1}.

gravitons (> 775 GeV). To improve the signal to background ratio there is a veto on isolated leptons. The irreducible SM backgrounds are $Z(\rightarrow \nu\nu)jj$ and $W(\rightarrow l\nu)jj$. The signal and background were generated with PYTHIA, which does not generate the two jets from matrix element calculations but with initial and final state QCD radiation and parton showering. Therefore the results contain a systematic error due to this approximation. The PDF used was CTEQ5L. The generated events went through the fast simulation and reconstruction of the ATLAS detector. The cascade decays were suppressed. On the other hand, the second KK level is kinematically suppressed and the proton top flavour content ignored.

Figure 11 shows the variation of the significance of the signal as a function of the mass of the first KK excitation state for 100 fb^{-1}. The 5σ discovery reach in ATLAS for 100 fb^{-1} is achieved for a first KK excitaion mass of 2.7 TeV.

3 Extra Gauge Bosons (Z', W')

3.1 Introduction

Extra Gauge Bosons are predicted by many different theories:

- Super-string inspired and Grand Unification theories (GUT).
- Left-Right Symmetric Models based on the gauge group $SU(3)_C x SU(2)_L x SU(2)_R x U(1)_{B-L}$ predicting substructures of the known elementary particles.
- Little Higgs Models.

There exist stringent limits from precision electro-weak experiments and direct searches. Those limits vary significantly from model to model because the different chiral couplings to the ordinary fermions predicted by them. Typically the $m_{Z'} \geq 400$ GeV and the Z-Z' mixing angle is below a few 10^{-3} for models in which the Z' couples significantly to charged leptons. On the other hand, for models with suppressed couplings to charged leptons the $m_{Z'} \geq$ 300-600 GeV and can tolerate much larger mixings (several %) but with the dominant constraint from the shift in the light Z mass.

At LHC should be possible to discover a heavy Z' with mass up to 5 TeV through its leptonic decay and should be possible to deeply study its couplings via F-B asymmetries, rapidity distributions, rare decays (Z' → Wlν) and associated productions with a Z, W or γ.

3.2 Experimental results

CMS results for pp → Z' → μμ [5,21]: the selection cuts to discriminate the signal from the background look for two opposite signed muons. The energy associated to the muon candidates is corrected for electromagnetic processes. The irreducible background is $Z \rightarrow \mu\mu$. Other backgrounds are ZZ, WZ, WW, tt\bar at the level of few % of the Drell-Yan and further suppressed with selection cuts. Other potential backgrounds like cosmic, jet-jet, W-jet, bb\bar, hadron punch through and poorly measured Z → μμ, have not been studied yet. Authors claim that they will be also negligible compared to Drell-Yan. The signal and backgrounds were generated with Pythia and include the full γ*/Z/Z' interference. Exotics decays are closed. The generated events were passed through the full simulation and reconstruction programs of CMS including low (5 events) and high (25 events) luminosity pile-up. The studied systematic uncertainties include theoretical and muon and tracker misalignment uncertainties.

Figure 12-left shows the integrated luminosity needed to discover with a 5σ significance several Z' masses. The significance calculation was done with the likelihood-ratio-based test statistics (unbinned) given by:

$$\mathcal{S}_{\mathcal{L}} = \sqrt{(2 \ln(\mathcal{L}_{S+B}/\mathcal{L}_B)} > 5 \qquad \text{(Eq. 7)}$$

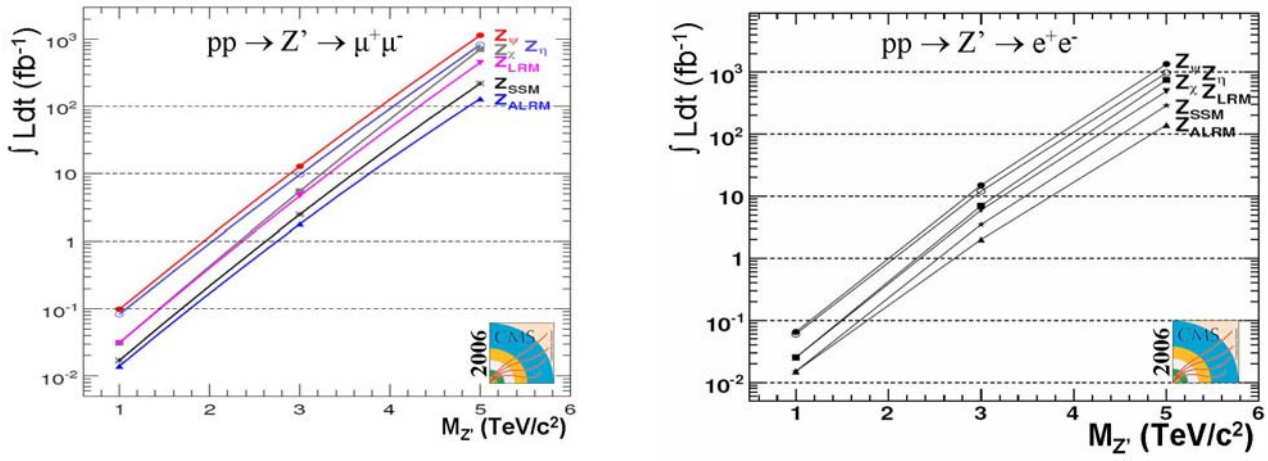

Figure 12: Integrated luminosity needed to discover with a 5σ significance several Z' masses for different heavy bosons theories: Zψ, Zη and Zχ arise in GUT; Z_{SSM} is the Sequential Standard Model; Z_{LRM} and Z_{ALRM} arise in the framework of Left-Right and Alternative Left-Right models. Symbols indicate fully-simulated-reconstructed mass-luminosity points, while lines are interpolations.

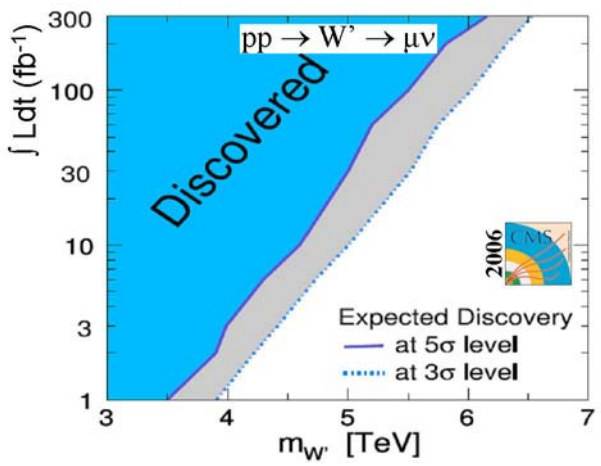

Figure 13: Integrated luminosity needed to discover with a 5σ significance several W' masses within the Reference Model by Altarelli.
The significance is calculated according to Eq. 4.

Without taking into account systematic uncertainties, an integrated luminosity < 0.1 fb^{-1} and non optimal alignment of the tracker and muon detectors, is enough to discover a Z' of 1 TeV (~ 50% less data is needed to reach the same signal significance if the optimal alignment is achieved). Ten fb^{-1} is sufficient to reach 5σ significance at ~ 3 TeV for most (but not all) the Z' models considered if the optimal alignment is achieved. Finally, 100 fb^{-1} doesn't allow to obtain 5σ significance at ~ 5 TeV with only the Z' → μμ channel for any of the models considered. The mass reach is between 3.9 TeV and 4.9 TeV.

CMS results for pp → Z' → ee [5,9:e+e-]: this analysis is the same as described in Sec. 2.4.2 (CMS results for pp → Z_1^{KK}/γ_1^{KK} → ee). Figure 12-right shows the integrated luminosity needed to discover with a 5σ significance several Z' masses.

CMS results for pp → W' → μν [22]: the topology of this process consists of an isolated and well identified muon with high p_T. The analysis was done at low luminosity with ~ 3 pile up events, using full simulation and reconstruction. CMS looks for charged spin-1 W' from the Reference Model by Altarelli. The irreducible background is $W \to \mu\nu$. Other backgrounds also studied are Z → μμ, WW, ZW and tt\bar.

Such a boson is expected to be discovered, if exists, with a mass up to 4.6 TeV for an integrated luminosity of 10 fb^{-1}. The range can be expanded to 6.1 TeV for 300 fb^{-1}. If no signs for a new W' boson appears, 95% CL exclusion limits of 4.7 TeV and 6.2 TeV can be set respectively.

4 How to discriminate between models

Once a resonance is discovered in the detector, the study of the angular distributions and the Forward-Backward asymmetry (A_{FB}) provide a way to investigate the nature of the new particles as it will be described in the following.

ATLAS discrimination method [13]: if a KK gauge excitation is discovered it can be distinguish from a Z' or from a narrow graviton resonance studying the angular distribution of the decay products (which should be consistent with the spin 1 nature of the excitation) and the A_{FB}. Figure 14 shows the mass distributions normalized to an integrated luminosity of 100 fb^{-1} for a Z_1^{KK}/γ_1^{KK} (M1 and M2 models), a Z' and a G_1^{KK} decaying into an electron pair. Events around the peak of the resonance are selected (3750 GeV < m_{ee} < 4250 GeV). For these events, the cosine of the angle of the lepton w.r.t. the beam direction, in the frame of the decaying resonance, is shown in Fig. 15. To compare the shape of these cosines, a set of 1000 angular distributions from the different type of resonances was generated by sampling from the expected distributions of Fig. 15. A Kolmogorov test was then applied between the expected Z_1^{KK}/γ_1^{KK} distribution and distributions sampled from the other resonances. The result of the test (Fig. 16) is expected to be uniformly distributed between 0 and 1 if they come from the same parent distribution. The biggest discriminating power is achieved for Z_1^{KK} versus G_1^{KK}. The test rejects with 95% CL the hypothesis that the distributions derive from the same parent distribution 91% of the times. A χ^2 test was also performed giving the same results.

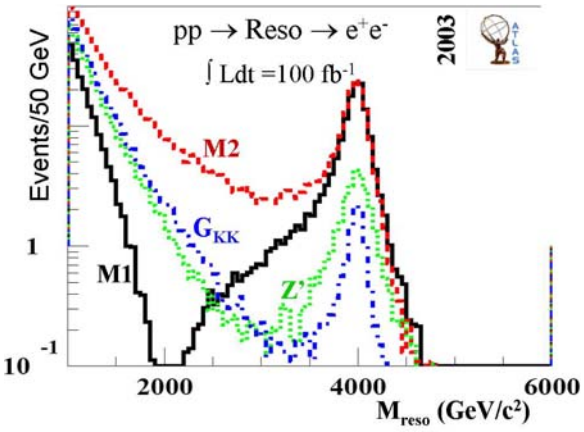

Figure 14: Invariant mass distributions normalized to an integrated luminosity of 100 fb^{-1} for a Z_1^{KK}/γ_1^{KK} (M1 and M2 models), a Z' and a G_1^{KK} decaying into an electron pair.

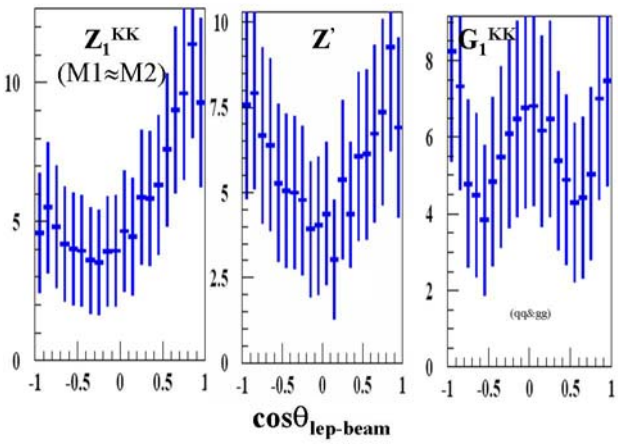

Figure 15: Cosine of the angle of the electron w.r.t. the beam direction, in the frame of the decaying resonance. The distributions are normalized to the number of events predicted for 100 fb^{-1} for the resonance Z_1^{KK}/γ_1^{KK}.

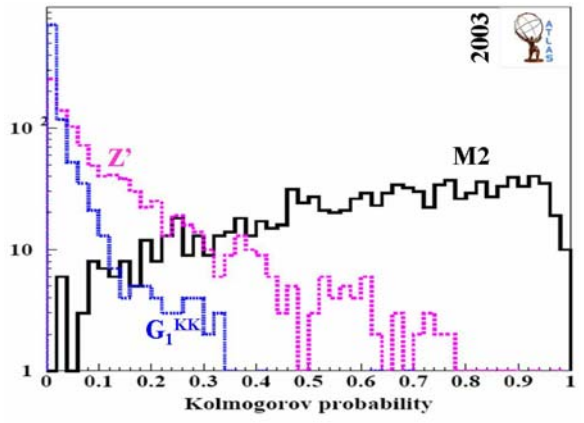

Figure 16: Kolmogorov probability from comparison of the different resonances. A histogram is constructed from 1000 pseudo samples of events.

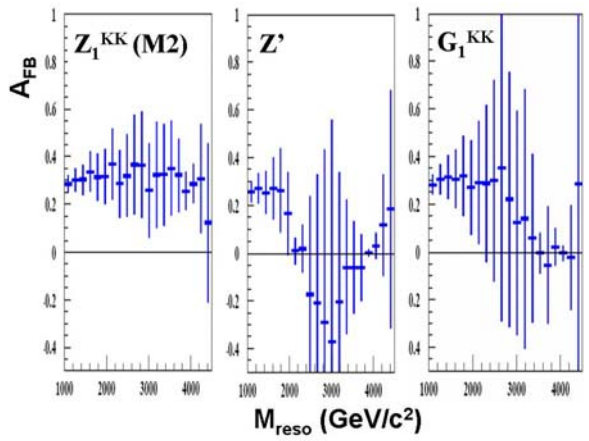

Figure 17: A_{FB} for the electron channel, for different types of resonances centred at 4 TeV.

From the angular distributions of Fig. 15, the A_{FB} for different types of resonances is obtained in Fig. 16 as a function of the reconstructed di-electron mass. As can be seen it allows for a clear discrimination between the models.

CMS discrimination method [5]: In order to distinguish the spins of a spin-1 Z' boson and a spin-2 gravitons in a di-lepton decay mode, CMS considers a unbinned likelihood ratio statistic incorporating the angles of the decay products as described in [23]. The statistical interpretation of this statistic is discussed in detail in

[24], which also considers the possibility of spin 0. The method has been applied to fully-reconstructed Z' and RS gravitons. Details of the simulation, trigger and reconstruction are given in [5].

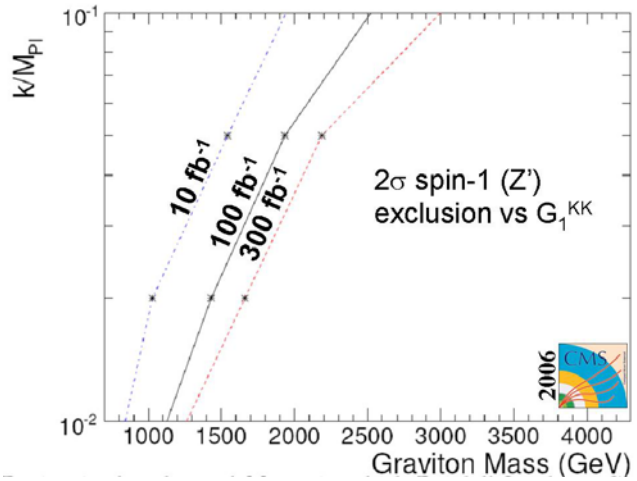

Figure 18: Region in the plane (c=k/$\mathbf{M_{Pl}}$,m(G_1^{KK})) where RS G_1^{KK} can be distinguished from Z' with 2σ significance if one treats the two spin hypothesis symmetrically. The region which can be probed lies to the left of the lines.

Figure 18 shows the region in the plane (c=k/$\mathbf{M_{Pl}}$,RS graviton mass) in which RS gravitons can be distinguished from Z' with 2σ significance if one treats two spin hypothesis symmetrically for a few representative values of the integrated luminosity. The results shown in the Figure correspond to the long term misalignment scenario and the Z' production cross section is assumed to be equal to that of the RS graviton with the given c value. Since the production cross section falls rather steeply with mass, the integrated luminosity needed for spin discrimination increases with mass. For RS gravitons the production cross section scales with c2, therefore, the integrated luminosity required for spin discrimination quickly increases as c gets smaller, and so does the number of signal events, because the larger the background contamination.

As discussed in [24], discriminating either spin-1 or spin-2 from spin-0 requires significantly more events than discriminating spin-2 from spin-1.

5 Conclusions

This conference report compiles the most recent results, from the experimental (simulation) point of view, on Extra Dimensions and Extra Gauge Bosons theories. In particular, the CMS and the ATLAS Collaborations analyses have been considered here. Almost all the analyses have included theoretical and experimental systematic errors in the discussion of the final results. The centre of mass energy considered has been 14 TeV with low and/or high luminosity scenarios. In general, the first year of data taking at high luminosity will allow discovering BSM signatures up to few TeV with a 5σ significance.

The conference report also addresses an extremely important subject: once a signature is discovered in the detector, how we can distinguish which model is the responsible for it. It has been demonstrated that thought the study of the angular distributions and the Forward-Backward asymmetry, the nature of the new particles can be disentangled.

References

[1] **Phys. Rev. D59, 086004 (1999),** N. Arkani-Hamed, S. Dimopoulos and G. R. Dvali.

[2] **Phys. Rev. Lett. 86 1156 (2001)**, B. Abbott et al. DØ Collaboration.

[3] **J. Phys. G: 27 (2001) no. 8, pp.1839-50**, L. Vacavant, I. Hinchliffe.

[4] **CMS NOTE 2006/129**, J. Weng, C. Saout, G. Quast, A. De Roeck, M. Spiropulu.

[5] **CERN/LHCC 2006-021,** CMS TDR 8.2 26 Jun 2006.

[6] **CMS NOTE 2005/002,** R. Cousins, J. Mumford, V. Valuev.

[7] **CMS NOTE 2006/076**, I. Belotelov et al.

[8] **Phys. Rev. Lett. 83 3370-3373 & 4690-4693 (1999),** l. Randall and R. Sundrum.

[9] **e+e- : CMS NOTE 2006/083**, R. Clerbaux, T. Mahmoud, C. Collard and P. Mine;

μ+μ- : CMS NOTE 2006/104, I. Belotelov et al.

γ γ : CMS NOTE 2006/051, M.-C. Lemaire, V. Litvin, H. Newman.

[10] **Phys. Rev. D63, 075004 (2001)**. Davoudiasl, Hewett, Rizzo.

[11] **CMS NOTE 2005/004**, V. Bartsch, G. Quast.

[12] **Nucl. Phys. B537 (1999) 47**, K. Dienes, E. dudas, T. Gherghetta;
Phys. Lett. B460 (1999) 176, I. Antoniadis, K. Benakli, M. Quiros.

[13] **Eur. Phys. J. C: 39 (2005) no. Suppl. 2, pp.1-11**, G. Azuelos and G. Polesello.

[14] **Eur. Phys. J., C 32 (2004) s55-s67**, G. Polesello and M. Prata.

[15] **ATL-PHYS-PUB-2006-002**, L. March, E. Ros and B. Salvachua.

[16] **Phys. Rev. D64, 035002 (2001)**, T. Appelquist, H. C. Cheng and B. A. Dobrescu.

[17] **Nucl. Phys. B 650, 391 (2003)**, G. Servant and T. Tait.

[18] **Physics at LHC Proceedings**, Krakow 3-7 July, 2006.

[19] **Proceedings of the Statistical Problems in Particle Physics, Astrophysics and Cosmology Conference**, PHYSTAT 05.S. I. Bitykov, S. F. Frofeeva, N. V. Krasnikov, A. N. Nikitenko;

[20] **ATL-PHYS-PUB-2005-003**, P. H. Beauchemin and G. Azuelos.

[21] **CMS NOTE 2006/062**, R. Cousins, J. Mumford, and V. Valuev.

[22] **CMS NOTE 2006/117**, C. Hof, T. Hebbeker and K. Hoepfner.

[23] **J. High Energy Phys. 09 (2000) 019**, B. C. Allanach, K. Odagiri, M. J. Palmer, M. A. Parker, A. Sabetfakhri, B. R. Webber.

[24] **JHEP 11 (2005) 046; doi:10.1088/1126-6708/2005/11/046,** R. Cousins, J. Mumford, J. Tucker, V. Valuev,